PAPER • **OPEN ACCESS**

Parametric optimization of non-prismatic micro-plates to reduce stiffening and curling initiated during fabrication

Parametric optimization of non-prismatic micro-plates to reduce stiffening and curling initiated during fabrication

B Bakeer[1], A Elsabbagh[1] and M Hedaya[1]

[1]Design and Production Engineering Department, Ain Shams University, Cairo, 11517 Egypt

Email: bahi.bakeer@eng.asu.edu.eg

Abstract. Microelectromechanical devices such as accelerometers, gyroscopes, pressure sensors, and radiofrequency (RF) switches are widely used in aerospace applications. Reduction of stiffening and curling initiated during fabrication of these devices is one of the challenging issues in MEMS design. Reducing response time is also favorable in some applications such as RF MEMS switches. This paper aims at reducing stiffening, curling, and increasing the natural frequency for three well-known designs of micro-plates with fixed-fixed supports. To achieve these objectives, a parametric size optimization is carried out. For comparison purposes, same volume is set as a constraint for all three designs. Compared to conventional rectangular micro-plate, a reduction of 34% in stiffening in design 2, and 44% in curling in design 3. Design 1 showed the maximum fundamental natural frequency. Thus, it is predicted to have the lowest switching time. Moreover, design 2 showed the maximum critical buckling temperature, extending the operation range of the device. The effect of changing micro-plate material is also studied in this paper.

1. Introduction

Microelectromechanical systems (MEMS) are used in wide variety of aerospace applications such as inertial navigation systems, structural health monitoring, and communication systems. Accelerometers, gyroscopes, pressure sensors , and radio-frequency (RF) MEMS switches are examples of devices used in these systems[1,2]. These devices have superior accuracy, light weight, low power consumption and lower cost than the macro-scale counterparts. The main research challenges facing the use of MEMS devices are related to their reliability and other performance parameters such as switching time in RF-MEMS switches. One of the main problems affecting the reliability of MEMS devices is the existence of residual stress due to fabrication processes [3]. The residual stresses cause two main problems 1) stress stiffening due the biaxial stress in axially restrained beams/plates, and 2) curling due to the stress gradient across the thickness. Both stress stiffening and curling affect the performance parameters of the MEMS devices.

Current technologies allow for different configurations for MEMS microplates. MEMS devices are fabricated either by surface micromachining or by bulk micromachining. In surface micromachining, the device is built on the surface of the substrate. Physical vapor deposition (PVD), chemical vapor deposition (CVD), and sputtering are examples of processes used extensively in surface

micromachining. On the other hand, the bulk micromachining processes done by etching the substrate at selected positions.

An example of MEMS device fabricated from microplates is RF MEMS switches. RF MEMS switches are extensively used in satellite systems, communication system networks, instrumentation, wide band spectral analysis and radar systems. These switches are used for control of radio frequency signals and signal routing [4]. Many switches are fabricated using surface micromachining processes by deposition and etching of different layers till the required design is implemented. Deposition techniques result in stress gradients in the switch resulting in stiffening and curling. Different deposition conditions of the top and bottom layers of the beam/plate are the reason behind this stress gradient [5]. Stiffening and curling in RF MEMS switches negatively affect their performance by increasing the needed voltage for actuation.

A lot of research was done to MEMS structures in order to improve their performance. Stress gradient causes considerable curling for devices in the form of cantilever beams. In addition, the performance of the device is affected by the non- symmetric orientation of the cantilever beam [6]. Fixed-Fixed beams [7] is less vulnerable to the stress gradient, but it usually experiences stress stiffening due to the residual in-plane stress. Joglekar and Pawaskar [8] optimized the micro-beam width profile in order to extend the static and dynamic travel range of cantilever and fixed-fixed beams. Shekhar et al.[9] studied previously known geometries of RF MEMS switches in order to enhance their dynamic characteristics. Peroulis et al. studied the effects of residual stress in RF MEMS switches and proposed methods to alleviate them [10]. Mahameed and Rebeiz developed a stable electrostatic RF MEMS capacitive switch based on a thermal buckle-beam design [11]. Gupta et al. reduced the out-of-plane warpage in micromachined beams using corrugation [12]. Nieminen et al. designed a temperature-stable RF MEMS capacitor. The design is based on a square micro-plate structure with slits at specific positions [6]. Demirel et al. developed RF MEMS shunt switches for special radio frequencies and studied their structure and fabrication [13,14]. Philippine et al. used topology optimization to minimize the stiffening and curling on capacitive RF MEMS switches [15]. Finally, Bansal et al. introduced reinforcement for reduced buckling in MEMS switches [16].

In this paper, three designs of fixed-fixed micro-plates reported in literature [9,17] are investigated. The objective is to minimize stress stiffening and curling arising from residual stresses. Two of the designs under investigation have stepped variation in thickness while the third one is characterized by gradual variation in thickness according to a parabolic function. Non-linear Finite Element plate model considering the midplane stretching and stress gradient is developed in order to capture the effects of the biaxial residual stresses. A parametric optimization to the ratio between the width of the plate at the mid-length to the width at the supports is done for all three designs. Stiffening, curling, and natural frequencies are computed. Constant volume is set as a constraint to all designs for fair comparison purposes. The effect of changing the material is also studied. The total stiffness versus the operating temperature is simulated in order to determine the critical buckling temperature.

The rest of this paper is organized as follows. Section 2 describes the three designs of the micro-plate. Section 3 represents the details of the developed Finite element model. The results are discussed in section 4. Conclusions and future work are stated in section 5.

2. Micro-Plate Design

2.1. Micro-Plate Configuration

The three designs under consideration with their main dimensions are shown in Figure 1. In the first and second designs, the width of the middle third of the micro-plate is different from the width at the support according to a step function. The third design has a parabolic width profile.

The overall length L, and thickness of all three designs are 200, 1 μm, respectively. The width at mid-length and at the anchors are denoted as W_1 and W_2, respectively. It is worth mentioning that for the first and third designs, W_1 is not necessarily larger than W_2, as will be shown in the next sections.

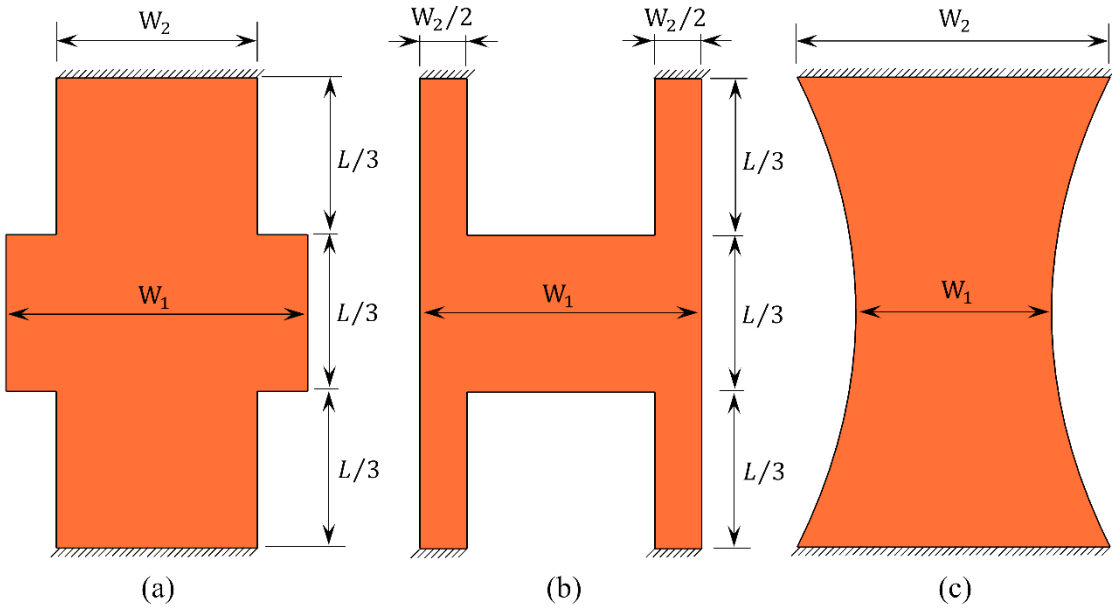

Figure 1. Schematic drawing of the three designs of the micro-plates**.**

2.2. Parametric optimization

To determine the effect of the widths W_1 and W_2 on mechanical performance of the micro-plates, a parametric optimization is carried out. Stiffening ratio, curling due to residual stresses, and the fundamental natural frequency are computed at different values of ratio a which is equals to W_1/W_2 . The ratio a ranges from 0.5 to 2 for designs 1 and 3, and ranges from 1 to 2 for design 2. The used materials and their main properties are shown in Table 1 [18,19]. For comparison purposes, the volume of the three designs is kept constant and equals to 20,000 μm^3, whatever the value of a.

Table 1. The used materials and their main properties.

	Young modulus E $10^9[N/m^2]$	**Poisson's ratio ν**	**Thermal expansion coefficient α 10^{-6}[1/K]**
Aluminum	77	0.3	23.1
Nickel	219	0.31	13.4
Gold	70	0.44	14.2

3. Finite Element Model of The Micro-Plate

The evaluation of the mechanical performance of the micro-plates is carried out by developing a 3D non-linear Finite Element plate model considering the midplane stretching and stress gradient developed using COMSOL Multiphysics.

Stiffening, curling, and natural frequencies are computed. Constant volume is set as a constraint to all designs for comparison purposes. The critical buckling temperature is determined by computing the stiffness versus operating temperature. All simulations are done with aluminum as a micro-plate material. Nickel and Gold are used only in stiffness versus temperature simulation. The details of each simulation are elaborated in the next subsections.

3.1. Stiffening and Curling

The micro-plate domain is meshed into triangular prism elements. The maximum and minimum element sizes are 4 and 0.04 μm, respectively. The actuation area is the lower surface of the micro-plate

A_{ac}=20,000 μm^2, taking into consideration the constant volume and thickness. The effective spring constant of the micro-plate is thus

$$k = \frac{p\, A_{ac}}{w_c} \tag{1}$$

where p is the force per unit area, and w_c is the deflection of the center point.
Stiffening is the ratio between the increase in stiffness due to the midplane stretching $\boldsymbol{k_2}$ to the stiffness without axial force $\boldsymbol{k_1}$. To calculate $\boldsymbol{k_1}$, a small force per unit area of 10 $\mathbf{N/m^2}$ is applied to the actuation area such that the non-linear effects are negligible. To calculate $\boldsymbol{k_2}$, the total stiffness is computed after applying the biaxial mean residual stress $\boldsymbol{\sigma_o}$. Hence, the stiffening ratio $\boldsymbol{k_2/k_1}$ can be calculated. The geometric non-linearity is included in the FE model to capture the coupling between the deflection and the midplane stretching. The total stiffness versus the operating temperature is simulated. This simulation is important to determine the critical buckling temperature for different designs and materials.

For simplicity, the substrate is not included explicitly in the model. The coefficient of thermal expansion CTE for the micro-plate is defined as the difference between CTE of the micro-plate material and alumina substrate (6.8 ppm/℃).
Curling is calculated when the micro-plate is subjected to the residual stresses $\boldsymbol{\sigma_{res}}$ without applying the actuation force such that

$$\boldsymbol{\sigma_{res}} = \begin{bmatrix} \boldsymbol{\sigma_o + \Gamma z} & \mathbf{0} & \mathbf{0} \\ \mathbf{0} & \boldsymbol{\sigma_o + \Gamma z} & \mathbf{0} \\ \mathbf{0} & \mathbf{0} & \mathbf{0} \end{bmatrix} \tag{2}$$

where $\boldsymbol{\Gamma}$ is the stress gradient across the thickness.
The values of $\boldsymbol{\sigma_o}$ and $\boldsymbol{\Gamma}$ are chosen similar to [18] to be 60 $\mathbf{MPa}$ and 10 $\mathbf{MPa/\mu m}$, respectively. Curling is calculated as the difference between maximum and minimum values of deflections of the whole micro-plate.

3.2. Natural Frequencies

The fundamental natural frequency f_o is computed considering the residual stress σ_{res} and geometrical non-linearity. The importance of this simulation is the relation between natural frequency and the switching time which is a key performance parameter in some MEMS devices such as RF MEMS switch. Equation (3) shows a simplified formula of the switching time [5]

$$t = 0.585 \frac{V_p}{f_o\, V_s} \tag{3}$$

where V_p and V_s are the pull-in and the applied voltages. This equation shows that the switching time is inversely proportional to the fundamental natural frequency f_o.

4. Results and Discussion

Figure 2 shows the stiffnesses k_1, k_2, and the total stiffness k_t versus the width parameter a for designs 1 (D1), 2 (D2), and 3 (D3). It is obvious that increasing a decreases all these stiffness components. This is attributed to the fact that the stiffness is more affected by the width at the anchor W_2 more than in the middle W_1. On the other hand, the stiffening ratio k_2/k_1 differs from design to another as shown in Figure 3. Figure 3 shows the stiffening ratio and curling versus the width ratio parameter a for all three designs. For the first and third designs (D1 and D3), the stiffening increases with the increase of a. The third design has a slight change. On the contrary, the stiffening ratio decreases with the increase of a for the second design (D2).

For design 1 and design 2, the minimum value of curling is found at a = 1 and a = 1.25, respectively. On the other hand, curling of design 3 increases with the increase of a. The second design has a negligible variation of curling with respect to a.

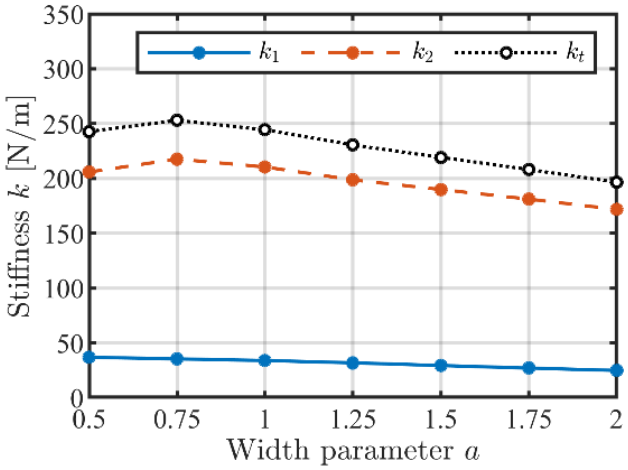

(a)

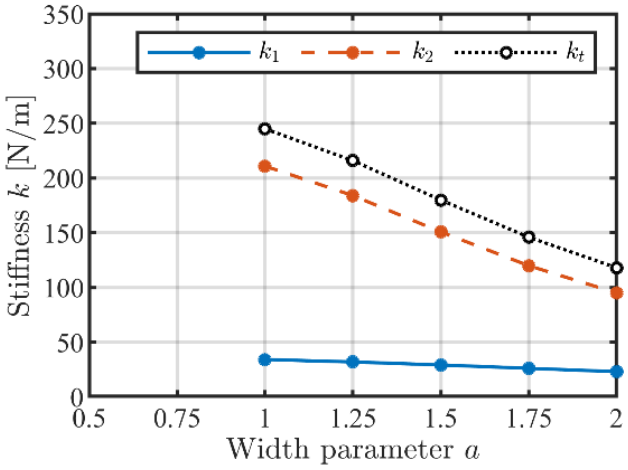

(b)

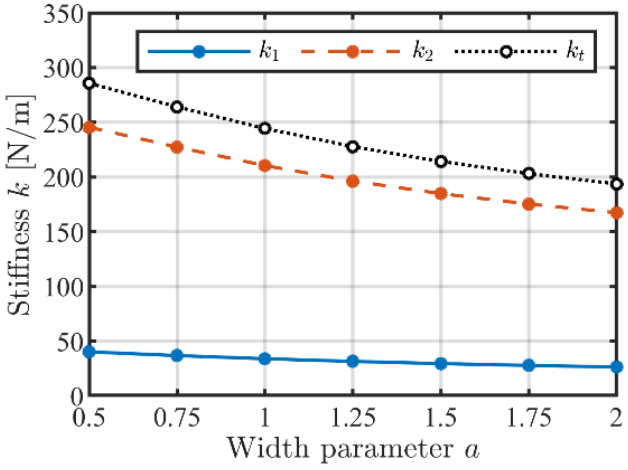

(c)

Figure 2. Stiffnesses k_1, k_2, and k_t versus the width parameter a for (a) Design1, (b) Design 2, and (c) Design 3.

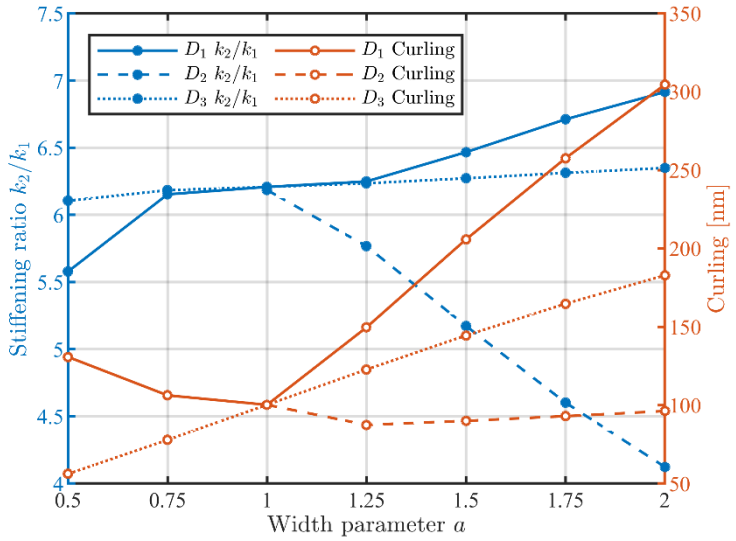

Figure 3. Stiffening and curling for the three designs versus the width parameter a.

The variation of the total stiffness with the operating temperature for the first design at a=0.5 and different types of materials is shown in Figure 4. Nickel (Ni) shows more stiffness than aluminum (Al) but both have close values of slope. Gold (Au) is less sensitive to temperature variation than Al and Ni. The variation of stiffness with temperature for all designs and materials are shown in Table 2.

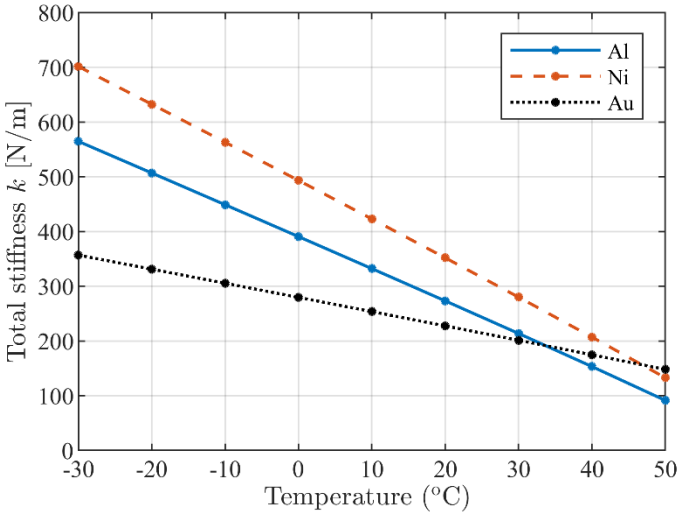

Figure 4. Total stiffness versus operating temperature for the first design at a=0.5 for different materials.

Table 2. Stiffness variation with temperature for all designs using different materials.

Stiffness variation with temperature [(N/m)/°C]								
Design 1			Design 2			Design 3		
Al	Ni	Au	Al	Ni	Au	Al	Ni	Au
-5.9	-7.1	-2.6	-2.4	-3.2	-1.1	-6.9	-8.5	-3.1

The second design (D2) shows the lowest variation. Thus, it has the highest critical buckling temperature. The critical buckling temperature is the temperature at which the bending stiffness of the plate vanishes. It is preferred to increase the critical buckling temperature to extend the operation temperature range of the MEMS device. Figure 5 shows the critical buckling temperature for all designs and materials at a=0.5 for D1 and D3, and at a=2 for D2.

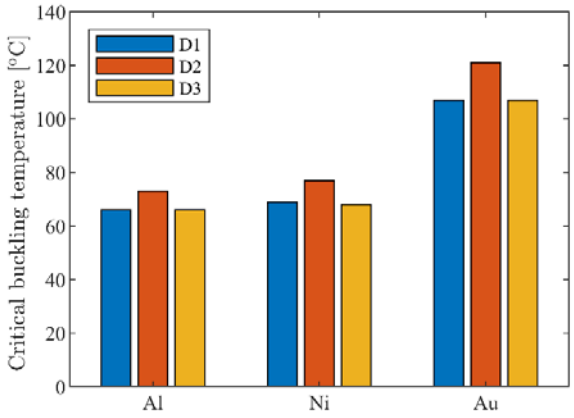

Figure 5. Critical buckling temperature for all designs and materials.

Figure 6 shows the fundamental natural frequency f_o versus the width ratio parameter a. Maximum f_o is found at minimum a for all designs. Design 1 shows higher f_o than design 3 at a less than 1. For higher values of a, the fundamental frequencies of design 3 are higher. The values of the fundamental natural frequency of design 2 coincides with that of design 1.

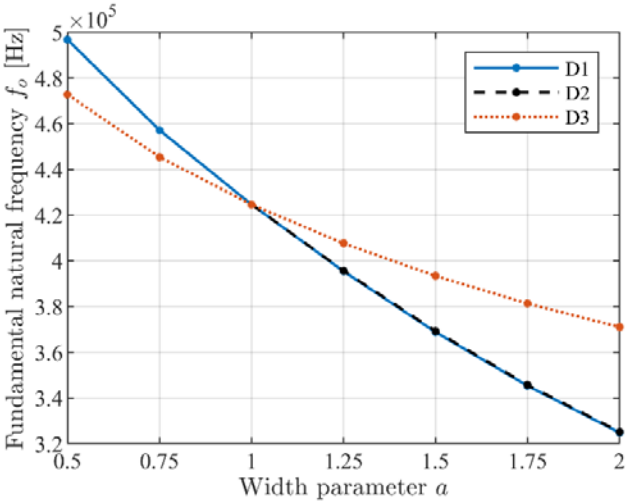

Figure 6. Fundamental natural frequency f_o for all designs and aluminum material versus width parameter a.

5. Conclusions

This work investigates the reliability issues related to residual stresses initiated during fabrication of MEMS devices in the form of micro-plates. The paper focuses on three well-known micro-plate designs found in literature. A parametric optimization for stiffening, curling, and fundamental natural frequency is carried out. The study variable a is the ratio between the width at the mid-length and the width at the supports. The first design has the highest natural frequency compared to other designs at the lowest a. Thus, this design can be used in applications that require high actuation speeds such as RF MEMS switches. The second design D2 has the lowest stiffening compared with other designs at the highest a. Thus, D2 has more stable operation with temperature variation. Moreover, it has a wider range of

operating temperatures due to its higher critical buckling temperature. The third design D3 has lower curling than the first and second designs at α=0.5. According to the specifications of the device and the fabrication process, one can select the required design. As a future work, experimental verification is needed to evaluate the performance of the proposed configurations. Moreover, topology optimization of a fixed-fixed plate for specific applications is also proposed.

References

[1] Osiander R, Darrin M A G and Champion J L 2006 MEMS and Microstructures in A erospace Applications (Boca Raton: CRC Press Taylor & Francis Group)
[2] Kraft M and White N M 2013 MEMS for Automotive and Aerospace Applications (Cambridge: Woodhead Publishing Limited)
[3] Saleem M M and Nawaz H 2019 A Systematic Review of Reliability Issues in RF-MEMS Switches *Micro Nanosyst.* **11** 11–33
[4] Rebeiz G M, Patel C D, Han S K, Ko C H and Ho K 2013 The search for a reliable MEMS switch? *IEEE Microw. Mag.* **14** 57–67
[5] Rebeiz G M 2003 *RF MEMS, Theory, Design, and Technology* (NewYork: Wiley)
[6] Nieminen H, Ermolov V, Silanto S, Nybergh K and Ryhänen T 2004 Design of a temperature-stable RF MEM capacitor *J. Microelectromechanical Syst.* **13** 705–14
[7] Goldsmith C L, Yao Z, Eshelman S and Denniston D 1998 Performance of Low-Loss RF MEMS Capacitive Switches *IEEE Microw. Guid. Wave Lett.* **8** 269–71
[8] Joglekar M M and Pawaskar D N 2012 Shape optimization of electrostatically actuated microbeams for extending static and dynamic operating ranges *Struct. Multidiscip. Optim.* **46** 871–90
[9] Shekhar S, Vinoy K J and Ananthasuresh G K 2017 Surface-Micromachined Capacitive RF Switches with Low Actuation Voltage and Steady Contact *J. Microelectromechanical Syst.* **26** 643–52
[10] Peroulis D, Pacheco S P, Sarabandi K and Katehi L P B 2001 Alleviating the Adverse Effects of Residual Stress in RF MEMS Switches *31st European Microwave Conference* (London, England)
[11] Mahameed R and Rebeiz G M 2010 A high-power temperature-stable electrostatic RF MEMS capacitive switch based on a thermal buckle-beam design *J. Microelectromechanical Syst.* **19** 816–26
[12] Gupta A, Barron L, Brainin M and Lee J B 2014 Reduction of out-of-plane warpage in surface micromachined beams using corrugation *J. Micromechanics Microengineering* **24** 065023
[13] Demirel K, Yazgan E, Demir S and Akin T 2016 A New Temperature-Tolerant RF MEMS Switch Structure Design and Fabrication for Ka-Band Applications *J. Microelectromechanical Syst.* **25** 60–8
[14] Demirel K, Yazgan E, Demir Ş and Akın T 2017 A folded leg Ka-band RF MEMS shunt switch with amorphous silicon (a-Si) sacrificial layer *Microsyst. Technol.* **23** 1191–200
[15] Philippine M A, Sigmund O, Rebeiz G M and Kenny T W 2013 Topology Optimization of Stressed Capacitive RF MEMS Switches *J. Microelectromechanical Syst.* **22** 206–15
[16] Bansal D, Bajpai A, Kumar P, Kaur M, Kumar A, Chandran A and Rangra K 2017 Low voltage driven RF MEMS capacitive switch using reinforcement for reduced buckling *J. Micromechanics Microengineering* **27** 024001
[17] Goldsmith C, Forehand D, Scarbrough D, Johnston I, Sampath S, Datta A, Peng Z, Palego C and Hwang J C M 2009 Performance of molybdenum as a mechanical membrane for RF MEMS switches *IEEE MTT-S International Microwave Symposium Digest* pp 1229–32
[18] Reines I, Pillans B and Rebeiz G M 2011 Thin-film aluminum RF MEMS switched capacitors with stress tolerance and temperature stability *J. Microelectromechanical Syst.* **20** 193–203
[19] Multiphysics C 2017 Comsol Multiphysics Library